

## Quantum-well band structure effects on the emission polarization from a spin-polarized electron reservoir

Mukul Agrawal and G. S. Solomon<sup>a)</sup>

*Solid State Photonics Laboratory, Stanford University, California 94305*

(Received 30 March 2004; accepted 25 June 2004)

Many spin-polarized-based devices utilize the optical polarization from semiconductor quantum wells (QWs) as a read out. Under ideal conditions at zero crystal momentum, 100% optical polarization is obtained from these QWs for fully polarized electrons. However, carrier populations typically extend over nonzero crystal momentum states, where band mixing results in nonideal optical polarization. We investigate a single  $\text{In}_x\text{Ga}_{1-x}\text{As}$  ( $x=0.2$ , and  $0.08$ ) QW in GaAs in a typical p-i-n spin injector structure, using eight band k.p theory including strain, electric field and quantum-confined Stark effects. By evaluating the carrier distribution and wave functions of the QW states, we find the resulting optical polarization is reduced to  $\sim 60\%$  at 10 K, and further for high temperature and high fields. We show that under certain conditions we can flip the sign of the optical polarization, suggesting the possibility of an electric field controlled optical or spin polarization switch. © 2004 American Institute of Physics. [DOI: 10.1063/1.1786373]

Semiconductor electronics has been built on the charge degree of freedom of electrons and holes. The spin degree of freedom, used in magnetic storage devices, has long been neglected in semiconductors. However, because of advances in semiconductor science and technology, control, and manipulation of the spin degree of freedom in semiconductors is becoming increasingly possible.<sup>1-5</sup>

The optical emission from a semiconductor quantum well (QW) structure is often used for spin detection of transported carriers through various materials and interfaces.<sup>6-8</sup> Ideal selection rules based on zone-center electron/hole wave functions are typically used to correlate the degree of emitted circular optical polarization with the degree of spin polarization.<sup>6,7,9</sup>

Here, we analyze the detailed carrier states in InGaAs/GaAs QWs of various alloy compositions starting from first principles. This analysis is not concerned with spin relaxation processes, focusing instead on the optical polarization emitted from a completely spin polarized electron population assuming a thermalized electron distribution in crystal momentum ( $k$ ) space. Using eight-band k.p theory with spin, we obtain the detailed wave functions and the corresponding eigenenergies for a few lowest lying bands of quasiconfined states under an applied electric bias across the structure. Variation in the carrier density among different energy and angular momentum states as a function of applied bias is then determined. We then investigate the radiative recombination of polarized electrons in the conduction band and unpolarized holes in the valence band via band to band optical transitions, and thus determine the degree of emitted circular polarization. We show that even at 10 K, the recombination dynamics deviate significantly from that predicted by simplified selection rules, and reduced the polarization of an  $\text{In}_{0.2}\text{Ga}_{0.8}\text{As}$  QW to 60%. Moreover, when an electric bias is applied the optical polarization goes to zero then switches sign.

We consider an undoped, 8 nm wide  $\text{In}_x\text{Ga}_{1-x}\text{As}$ -GaAs QW on (001) GaAs surrounded by  $p$ - and

$n$ -doped GaAs regions and injected with completely spin polarized electrons from the  $n$  side.  $p$ - and  $n$ -doping concentrations are  $5 \times 10^{18}$  and  $5 \times 10^{16} \text{ cm}^{-3}$ , respectively. The lightly  $n$ -doped region models an electron spin injector.<sup>6</sup> The QW indium compositions of 8% and 20% are chosen to investigate the effects of strain and quantum confinement on the polarization of emitted light.

Consider the InGaAs-GaAs QW with a constant electric field ( $E$ ) applied along the growth direction. An eight band k.p method,<sup>10-12</sup> typically used in strained bulk semiconductor systems, is used here to obtain the QW bound stationary states. Under the slowly varying envelope approximation,<sup>11,12</sup> the wave functions for each valence band quasibound state are written as the sum of four unstrained, bulk zone-center until cell functions,  $|u_{0i}\rangle$ , each modulated by an envelope wave function,  $F$ .<sup>11,12</sup> For each set of in-plane Bloch wave vector  $(k_x, k_y)$  and  $E$ ,  $F$  is obtained as solution of the matrix equation  $H_{QW}F = EF$ . The QW Hamiltonian,  $H_{QW}$  is obtained by replacing  $\hbar k_z$  by  $-\hbar \partial / \partial z$ <sup>11</sup> in the Hamiltonian for the bulk semiconductor which includes the biaxial strain effects through the Pikus-Bir formulation.<sup>13</sup> Effects of other higher energy bands are included indirectly through Luttinger parameters by way of the traditional Lowdin renormalization.<sup>14,15</sup>

This matrix equation is solved through the transfer matrix approach where the QW structure is divided into sufficiently small sections so that within each section the potential can be approximated to be constant. Enforcing the boundary conditions<sup>12</sup> between all the sections we obtain eight possible values of  $k_z$  and the corresponding eighteigenvectors. Through block diagonalization, we obtain two envelope wave functions, indexed  $i$ . We then solve for the four lowest valence band quantized energy states, indexed  $j$ , for different in-plane crystal momentum spanning about 10% of the first Brillouin zone and for different values of bias. The valence band wave functions are then written as  $|\psi_{v,j}\rangle = \sum_i F_j^i |u_{0,i}\rangle$ . Analogously, the wave functions and the corresponding eigenenergies for the two spin degenerate conduction bands were obtained by solving the single band effective mass equation using the same transfer matrix approach. The

<sup>a)</sup>Electronic mail: solomon@stanford.edu

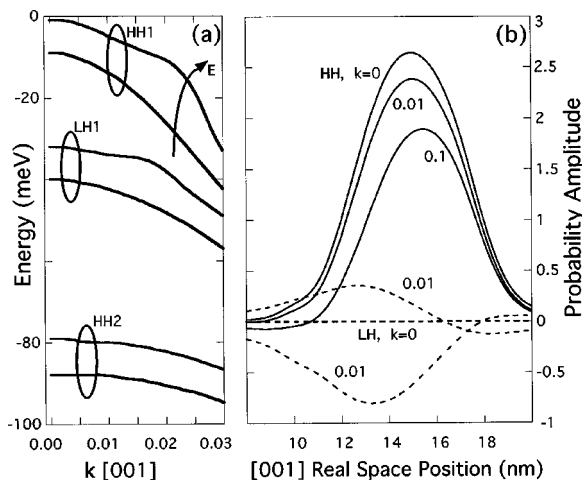


FIG. 1. (a) In<sub>0.2</sub>Ga<sub>0.8</sub>As heavy (HH1,2) and light (LH1) hole quasibound states for fields of 0 (lower) and 2 (upper) MV/m across the QW. Energies are referenced to the InGaAs unstrained, bulk valence band edge; (b) envelope functions corresponding to the two zone center unit cell functions for three different quasibound states  $k_x=0$ ,  $k_x=0.01$ , and  $k_x=0.1$ . Distances are referenced to the barrier edge.

wave function for the lowest conduction band,  $c$  is written as  $|\psi_c\rangle = F_c|u_{0,c}\rangle$  where  $|u_{0,c}\rangle$  is the bulk conduction-band zone-center unit-cell function.

The calculated bands of bound of stationary states for the In<sub>0.2</sub>Ga<sub>0.8</sub>As QW structure are shown in Fig. 1(a) for two different values of  $E$  (0 and 2 MV/m). The calculated valence band envelope functions are shown for three different values of crystal momentum in Fig. 1(b). as the bias or the crystal momentum increases, the nonparabolicity of the bands and the band mixing increases. Also, the quantum confined Stark shift is evident: the shift in the energy increases as the bias across the QW increases and the real space position of the envelope function changes [Fig. 1(b)].

To determine the variation in the carrier distribution among the bands in  $k$  space inside the QW as the electric bias across the structure is varied, a commercial simulator, Atlas, was used, assuming a thermalized quasi-Fermi distribution. The resulting electron and hole quasi-Fermi levels were then used to calculate the crystal momentum and sub-band distribution of the carriers.

The relative flux of right (RCP) and left (LCP) circularly polarized photons with electric field vector in the QW plane is:

$$f_{\text{RHCP}} = \frac{(P_{cv}^2/4)}{(LHCP)} \int_k f[E(k)] n_{\text{RHCP}} dk,$$

where

$$n_{\text{RHCP}} = \sum_f \int_z \left| F_j^{(ih)} F_c^{hh} \right|^2 dz$$

are related to the conduction and valence band wave function overlaps,  $p_{cv} = \langle u_{0,c} | -i\hbar \nabla_{x,y} | u_{0,h} \rangle$  is the momentum matrix element between the conduction and valence zone center unit cell functions and  $f[E(k)]$  is the quasi-Fermi distribution function;  $\nabla_{x,y}$  is the in-plane component of spatial gradient.

Figure 2 shows the variation of the relative optical polarization as the electric field is varied. Even with our assumption of preserved spin orientation in the QWs and with

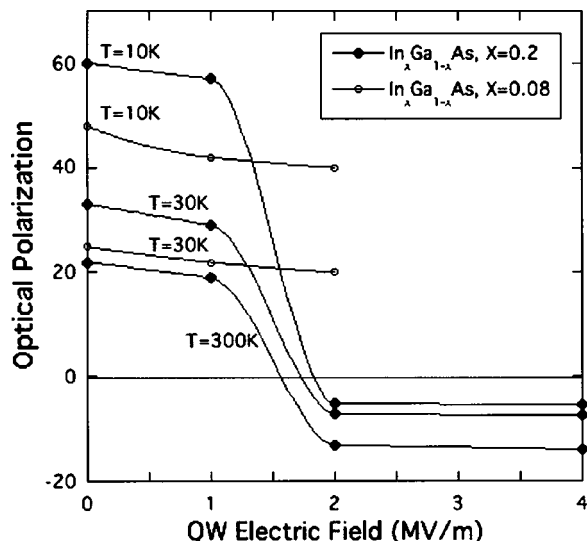


FIG. 2. Percentage circular optical polarization as a function of applied electric field across the InGaAs/QW, for three temperatures ( $T=10, 30$ , and  $300$  K) and two In compositions (0.08 and 0.20). Lines are a guide to the eye.

no electrical bias, the emitted polarization is significantly less than 100% at 10 K. 100% circular polarization only occurs from recombination of zone-center electrons and holes. Since carriers occupy a distribution of states, the electron-hole recombination from nonzone-center states produces photons of mixed polarization, and the relative polarization of the total emitted radiation is always expected to be less than 100%. In addition, there is a small contribution due to an approximate 5% LH band occupation. As the electric field is increased, the LH envelope function increases in magnitude in the HH band, and the momentum matrix elements associated with opposite polarization grows. In fact, as the field increases, the sense of circular polarization of emitted radiation switches. This may be useful as a polarization switch either flipping the sign of spin polarization under optical pumping or flipping the sense of optical circular polarization under polarized spin injection. Figure 2 also shows the expected temperature variation of the optical polarization. At lower temperatures there is very little carrier population in the LH band, and the distribution of carriers in  $k$  space is confined very close to the zone center. As temperature increases, carriers spread farther in the Brillouin zone, as well as into the LH band, reducing the emitted peak optical polarization. Because contributions from more than one band become more significant at higher at higher temperatures, not only does the peak polarization decrease but so does the overall change in polarization with field. Finally, Fig. 2 shows the variation of optical polarization as the In composition is varied. Because of weaker confinement at lower In concentrations the separation of valence band states is reduced, increasing valence band mixing away from  $k=0$  and thus reducing the optical polarization. Furthermore, with a smaller In composition it is not possible to maintain the QW confinement under high electric field. In practice, higher In content QWs may lead to lower optical polarization because of less ideal QW interfaces and spin scattering dynamics; however, these effects are not included in this model.

In conclusion, the spin recombination dynamics in InGaAs QWs are analyzed assuming a 100% spin polarized electron population, unpolarized hole population, thermalized

zed carriers, and no spin scattering. We concluded that even at low temperature and no electrical bias the correlation between emitted circular polarization and the spin polarization was less than the ideally assumed 100%. As the temperature or the electric field is increased, the calculated optical polarization further decreased.

The authors would like to acknowledge helpful discussions with X. Jiang at the IBM Research Laboratory, Almaden. This work was partially supported through the DARPA SPINS Program, through IBM Subcontract No. A0032300.

<sup>1</sup>S. Datta and B. Das, Appl. Phys. Lett. **56**, 665 (1990).

<sup>2</sup>H. Ohno, Science **281**, 951 (1998).

<sup>3</sup>J. M. Kikkawa and D. D. Awschalom, Nature (London) **397**, 139 (1999).

<sup>4</sup>R. Fiederling, M. Keim, G. Reuscher, W. Ossau, G. Schmidt, A. Waag, and L. W. Molenkamp, Nature (London) **402** 787 (1999).

<sup>5</sup>S. A. Wolf, D. D. Awschalom, R. A. Buhrman, J. M. Daughton, S. Von Mohr, M. L. Roukes, A. Y. Chtchelkanova, and D. M. Treger, Science **294**, 1488 (1992).

<sup>6</sup>X. Jiang, R. Wang, S. van Dijken, R. Shelby, R. Macfarlane, G. S. Solomon, J. Harris, and S. S. Parkin, Phys. Rev. Lett. **90**, 256603 (2003).

<sup>7</sup>H. J. Zhu, M. Ramsteiner, H. Kostial, M. Wassermeir, H. P. Schonerr, and K. H. Ploog, Phys. Rev. Lett. **87**, 016601 (2001).

<sup>8</sup>B. T. Jonker, A. T. Hanbicki, Y. D. Park, G. Itskos, M. Furis, G. Kioseoglou, A. Petrou, and X. Wei, Appl. Phys. Lett. **79**, 3098 (2001).

<sup>9</sup>A. T. Hanbicki, B. T. Jonker, G. Itskos, G. Kioseoglou, and A. Petrou, Appl. Phys. Lett. **80**, 1240 (2002).

<sup>10</sup>E. O. Kane, *Semiconductors and Semimetals*, edited by R. K. Willardson and A. C. Beer (Academic, New York, 1966), Vol. 1.

<sup>11</sup>S. L. Chuang, Phys. Rev. B **43**, 9649 (1991).

<sup>12</sup>L. C. Andreani, A. Pasquarello, and F. Bassani, Phys. Rev. B **36**, 5887 (1987).

<sup>13</sup>G. E. Pikus and G. L. Bir, Sov. Phys. Solid State **1**, 502 (1960).

<sup>14</sup>J. M. Luttinger and W. Kohn, Phys. Rev. **97**, 869 (1955).

<sup>15</sup>J. Singh, in *Handbook on Semiconductors*, 2nd ed., edited by T. S. Moss (Elsevier, Amsterdam), Vol. 2, p. 235.